Third-order magnetic susceptibility as a new method for studying quadrupolar interactions in rare-earth compounds

P. Morin and D. Schmitt

Laboratoire Louis Néel, Centre National de la Recherche Scientifique, 166X,
38042 Grenoble-Cèdex, France
(Received 24 December 1980)

We present a new method based on the detailed analysis of the magnetization curve in the paramagnetic range for studying the quadrupolar interactions in cubic rare-earth intermetallic compounds; the third-order magnetic susceptibility characterizes the anisotropic curvature of the magnetization curve. It corresponds to the H^3 coefficient in the odd field development of the magnetization. This high-order coefficient receives a contribution from the induced quadrupolar moment which varies as H^2. Thus studied in the nonordered (cubic and paramagnetic) range with magnetic fields applied along the [001] and [111] directions, the third-order magnetic susceptibility provides information on the quadrupolar interactions associated with the two tetragonal and trigonal symmetry-lowering modes. Using perturbation theory and mean-field approximation, we give analytical expressions for the third-order magnetic susceptibility in the presence of a crystalline electric field, bilinear exchange, and quadrupolar (exchange and magnetoelastic) interactions. Application to Tm^{3+} cubic intermetallic compounds, for which large quadrupolar interactions have been shown to exist, is then given, illustrating the reliability of the method.

I. INTRODUCTION

The magnetic properties of the cubic rare-earth intermetallic compounds have been extensively studied for the last few years, especially the magnetization processes. Because of the strong mixing of the $4f$ wave functions $|J,M_J\rangle$ by the crystalline electric field (CEF), the classical description of the magnetization fails and one finds at low temperature an anisotropic reduction of the magnetic moment in comparison with the free-ion value. This anisotropy of the magnetization occurs in addition to the anisotropy of the energy, which sets both the easy magnetization direction and the process of the rotation of the moment towards the magnetic field applied along a hard magnetization axis. The complete description of the magnetization processes then requires the diagonalization of the full Hamiltonian, including the CEF, the Zeeman coupling, and the bilinear Heisenberg exchange between the $4f$ ions. As a consequence such an analysis of the magnetization processes had allowed a determination, albeit rough, of the CEF parameters in many compounds.

However, it became rapidly apparent that the simple assumption of only bilinear exchange interactions in presence of CEF was too approximate: there exists strong magnetoelastic couplings between the $4f$ ions shell and its surroundings as well as higher rank exchange interactions such as the quadrupolar ones.[1] These quadrupolar exchange interactions are strong enough in a few cases to induce a quadrupolar ordering in absence of bilinear exchange interactions as in TmCd,[2] or above the magnetic ordering as in TmZn.[3]

In the other more usual cases the quadrupolar interactions are less strong than the bilinear ones, which then drive the magnetic ordering, but the quadrupolar interactions, nonetheless, deeply modify the magnetic properties, especially the magnetic moment and the anisotropy of the energy.[4]

In order to study the magnetoelastic coupling and the quadrupolar exchange interactions in presence of CEF and bilinear interactions and to separate their respective effects, it is necessary to carefully undertake specific experiments such as elastic constants[5] and parastriction[6] measurements. Carried out in the nonordered (cubic and paramagnetic) range they may be analyzed using perturbation theory methods: this allows us to eliminate (or minimize) the specific difficulties related to the exchange model and to have analytical expressions for the various susceptibilities connecting the involved variables, for instance: (1) the usual (first-order) magnetic susceptibility which couples the magnetization and the magnetic field, (2) the strain susceptibility, i.e., the response of the quadrupolar moment to the corresponding strain, which is used in the elastic constants analysis,[5,7] (3) the quadrupolar field susceptibility, connecting the quadrupolar moment to the square of the magnetic field, which appears in the parastriction.[6]

As a new way for studying the quadrupolar interactions, we want now to present the third-order magnetic susceptibility, which consists in a detailed analysis of the magnetization induced by an external field in the paramagnetic range. As the magnetization is an odd function of the magnetic field, the second term (in H^3) of its development is modified

by the quadrupolar contribution (in H^2). This then provides a new experimental method for investigating the quadrupolar interaction.

Section II is devoted to the derivation of the analytical expressions for the third-order susceptibility using a perturbation theory. If the first-order magnetic susceptibility is isotropic in cubic CEF, the third-order one is anisotropic leading to the anisotropy of the magnetization. Applying a magnetic field successively along fourfold and threefold axes allows one to separately determine the quadrupolar coefficients associated with tetragonal and trigonal symmetries. In Secs. III and IV we present illustrations of the method used on thulium compounds having the CsCl-type structure. The quadrupolar coefficients are then compared with determinations from other experiments (parastriction and elastic constants).

II. THEORY

A. Perturbation theory

The Hamiltonian used for describing the properties of the $4f$ shell in a cubic CEF has been extensively described in the recent past, in particular, in Ref. 6. It is developed by using the operator equivalent method and the mean-field approximation for the

description of the Heisenberg and quadrupolar exchange terms. The one-ion magnetoelastic coupling is restricted to the first term (proportional to the second-order Stevens operators) and the elastic variables are treated in the harmonic approximation.

Two types of order parameters are in presence: the magnetic moment, $\vec{M} = g_J\mu_B\vec{J}$ and the quadrupolar moments

$$Q = \langle O_2^0 \rangle = \langle 3J_z^2 - J(J+1) \rangle$$

for the tetragonal symmetry, and

$$Q' = \langle P_{ij} \rangle = \langle \tfrac{1}{2}(J_iJ_j + J_jJ_i) \rangle$$

for the trigonal ones. For instance, when the magnetic field H is applied along [001], only $\langle J_z \rangle$ and Q are nonzero and the full Hamiltonian is reduced to

$$\mathcal{K} = \mathcal{K}_{CEF} - g_J\mu_B(H + nM)J_z - B_1\epsilon_3 O_2^0 - K_1 Q O_2^0$$

$$+ [\tfrac{1}{2}(C_{11}^0 - C_{12}^0)(\epsilon_3)^2 + \tfrac{1}{2}nM^2 + \tfrac{1}{2}K_1 Q^2] \quad , \quad (1)$$

where n and K_1 are the bilinear and quadrupolar exchange coefficients, B_1 and $C_{11}^0 - C_{12}^0$ the magnetoelastic coefficient and the background elastic constant associated with the tetragonal strain $\epsilon_3 = 2\epsilon_{zz} - \epsilon_{xx} - \epsilon_{yy}$. Carried to second order in ϵ_3 and the fourth order in H, the perturbation theory leads to the expression of the free energy

$$F_{tot} = F_{CEF} - \tfrac{1}{2}\chi_0^{(1)}(H + nM)^2 - \tfrac{1}{2}\chi_2(B_1\epsilon_3 + K_1Q)^2 - \chi_2^{(2)}(B_1\epsilon_3 + K_1Q)(H + nM)^2$$

$$- \tfrac{1}{4}\chi_0^{(3)}(H + nM)^4 + \tfrac{1}{2}(C_{11}^0 - C_{12}^0)\epsilon_3^2 + \tfrac{1}{2}nM^2 + \tfrac{1}{2}K_1Q^2 \quad , \tag{2}$$

where four pure CEF susceptibilities may be calculated from the cubic CEF level scheme (Appendix A): $\chi_0^{(1)}$ is the well-known (first-order) magnetic one, χ_2 is the strain susceptibility involved in the ultrasonic velocity calculations,[5] $\chi_2^{(2)}$ is the quadrupolar field susceptibility appearing in the parastriction[6] and $\chi_0^{(3)}$ is the CEF third-order magnetic susceptibility. From the equilibrium conditions, the equilibrium values are then deduced:

$$M = \chi_M^{(1)}H + \chi_M^{(3)}H^3 \cdots \quad , \tag{3}$$

$$\epsilon_3 = \frac{B_1}{C_{11}^0 - C_{12}^0}Q \quad , \tag{4}$$

$$Q = \chi_Q H^2 \cdots \quad , \tag{5}$$

with

$$\chi_M^{(1)} = \frac{\chi_0^{(1)}}{1 - n\chi_0^{(1)}} \quad , \tag{6}$$

$$\chi_M^{(3)} = \frac{\chi_0^{(3)}}{(1 - n\chi_0^{(1)})^4} + 2G_1\frac{(\chi_2^{(2)})^2}{(1 - n\chi_0^{(1)})^4(1 - G_1\chi_2)} \quad , \tag{7}$$

$$\chi_Q = \frac{\chi_2^{(2)}}{(1 - n\chi_0^{(1)})^2(1 - G_1\chi_2)} \quad . \tag{8}$$

As it is well known in the mean-field approximation, the actual susceptibilities result from the enhancement of the corresponding CEF ones by the exchange interactions: in the case of the bilinear ones $n = \Theta^*/C$ with $C = g_J^2\mu_B^2 J(J+1)/3$, the Curie constant and Θ^* would be the paramagnetic Curie temperature in absence of CEF effects. In the case of quadrupolar interactions, $G_1 = B_1^2/(C_{11}^0 - C_{12}^0) + K_1$, the total quadrupolar coefficient, characterizes the sum of the magnetoelastic and quadrupolar exchange contributions. One finds again that the first-order magnetic susceptibility [Eq. (6)] depends only on the bilinear interactions; the quadrupolar field susceptibility [Eq. (8)] is reinforced by both the bilinear exchange (enhancing the applied field effects) and the quadrupolar interactions (enhancing the induced strain) and is involved in the parastriction process.[6]

Equation (7) shows that the total third-order magnetic susceptibility consists in two contributions, both strengthened in an identical manner by the bilinear interactions: (i) The first one corresponds to the CEF initial curvature, $\chi_0^{(3)}$, of the magnetization curve. Depending only on the level scheme as $\chi_0^{(1)}$,[8] and χ_2,[5] it is characteristic of this level scheme and provide an experimental determination of it. (ii) The

second contribution is the quadrupolar one. According to their relative sign, a competition between both contributions can be expected in some cases.

When the magnetic field is applied along the threefold axis, analogous calculations may be performed, their results are given in Appendix B.

B. Behavior of the third-order magnetic susceptibilities

1. Without CEF effect

When the CEF has no effect, the $4f$ ground-state multiplet (L,S,J) is completely degenerate. This $2J+1$ degeneracy leads to the well-known expressions for the first-order magnetic susceptibility (Fig. 1, left part)

$$\chi_0^{(1)} = \frac{C}{T} \tag{9}$$

without bilinear exchange and

$$\chi_M^{(1)} = \frac{C}{T - \Theta^*} \tag{10}$$

in presence of bilinear exchange interactions of strength Θ^* ($\Theta^* > 0$ for a ferromagnetic coupling).

$\chi_M^{(1)}$ diverges at the ferromagnetic Curie temperature $T_c = \Theta^*$ in the mean-field model.

In the same way, the curvature of the magnetization curve is defined in absence of any interaction by the third-order susceptibility (left part of Fig. 1)

$$\chi_0^{(3)} = \frac{C^{(3)}}{T^3} , \tag{11}$$

where $C^{(3)}$ is the third-order Curie constant

$$C^{(3)} = -g_J^4 \mu_B^4 \frac{J(J+1)(2J^2+2J+1)}{90} . \tag{12}$$

Note that $C^{(3)}$ is the negative H^3/T^3 coefficient in the development of the Brillouin function and that the third-order susceptibility is here isotropic.

In presence of pure bilinear exchange, the third-order susceptibility is reinforced:

$$\chi_M^{(3)} = \frac{C^{(3)}}{T^3(1-\Theta^*/T)^4}$$

diverges at $T_c = \Theta^*$, but the low-temperature behavior of $\chi_M^{(3)-1/3}$ is not linear. A third-order paramagnetic Curie temperature, $\Theta_p^{(3)} = \frac{4}{3}\Theta^*$, may be defined from the $\chi_M^{(3)-1/3}$ high-temperature extrapolation (Fig. 1, left part).
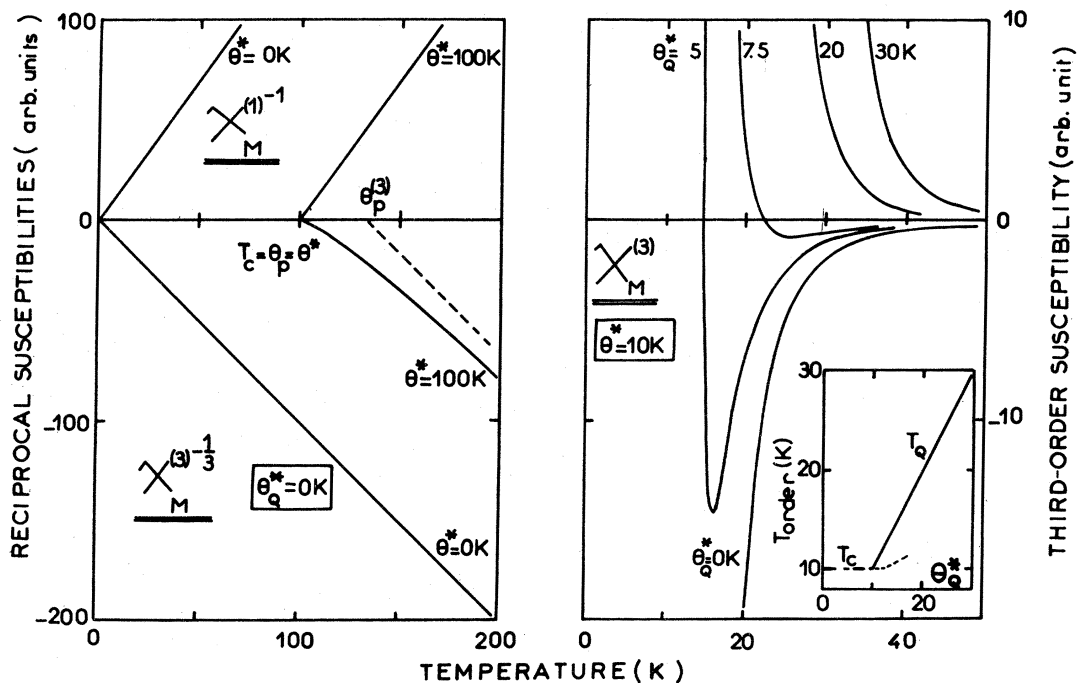
FIG. 1. Left part: Temperature behavior of the classical reciprocal first- and third-order magnetic susceptibilities without quadrupolar interactions ($\Theta_Q^* = 0$). Θ_p and $\Theta_p^{(3)}$ are the first- and third-order paramagnetic Curie temperatures, Θ^* characterizes the Heisenberg interactions, and T_C is the ferromagnetic Curie temperature. Right part: Temperature variations of the classical third-order susceptibility for various quadrupolar interactions and constant ($\Theta^* = 10$ K) bilinear interactions. The inset shows the phase diagram (——— T_Q, – – – T_C in the tetragonal phase, and —·— $T_C = T_Q$).

In presence of quadrupolar interactions the strain susceptibility X_2 and the quadrupolar field susceptibility $X_2^{(2)}$ occur. In absence of CEF effects, they reduce to the following isotropic expressions[6]:

$$X_2 = \frac{1}{5T} J(J+1)(2J-1)(2J+3) = \frac{C_Q}{T} , \quad (13)$$

$$X_2^{(2)} = \frac{1}{6} g_J^2 \mu_B^2 \frac{C_Q}{T^2} . \quad (14)$$

Let us define $\Theta_Q^* = C_Q G_1$ that leads to the following isotropic expression

$$X_M^{(3)} = \frac{C^{(3)}}{T^3 (1 - \Theta^*/T)^4}$$

$$\times \left[1 - \frac{(2J-1)(2J+3)}{2J^2 + 2J + 1} \frac{\Theta_Q^*}{T - \Theta_Q^*} \right] . \quad (15)$$

Thus, owing to the presence of both Θ^* and Θ_Q^*, the temperature dependence of $X_M^{(3)}$ may be very different (Fig. 1, right part). Instead of remaining always negative in all the temperature range as for $\Theta_Q^* = 0$ K, $X_M^{(3)}$ becomes positive at a threshold temperature $T_0 = (1 + \alpha)\Theta_Q^*$ with

$$\alpha = \frac{(2J-1)(2J+3)}{(2J^2 + 2J + 1)} ,$$

as soon as Θ_Q^* is nonzero. According to the relative strength of Θ_Q^* and Θ^*, various phase transitions may occur: (i) For Θ_Q^* smaller than Θ^*, the ferromagnetic ordering occurs at $T_c = \Theta^*$, driving the quadrupolar ordering too. All the magnetic susceptibilities [Eqs. (6), (7), (8)] diverge at T_c, the divergence of $X_M^{(3)}$ being negative for $T_c > T_0$ and positive for $T_c < T_0$. (ii) For Θ_Q^* larger than Θ^*, the quadrupolar ordering occurs at $T_Q = \Theta_Q^*$, where $X_M^{(3)}$ and X_Q diverge but not $X_M^{(1)}$. The magnetic dipoles are not ordered at T_Q; Θ^* drives their ordering at a lower temperature in the quadrupolar range according to the new level scheme.

2. With CEF effects and without quadrupolar interaction

The same high-temperature behaviors are found for all the susceptibilities, but additional effects may be induced at low temperature by the specific character of the low-lying CEF levels. As an example we discuss here the case of the trivalent thulium ion ($J = 6$), which provides, in cubic symmetry, the three possible configurations [Fig. 2(a)]: (i) a magnetic and quadrupolar ground state, as the triplet $\Gamma_5^{(1)}$ found for instance for the CEF parameters $W = 1.2$ K and $x = -0.31$ in the Lea, Leask, and Wolf's formal-

ism,[9] (ii) a nonmagnetic, but quadrupolar ground state: the Γ_3 doublet defined by $W = 2.2$ K and $x = -0.8$, (iii) a nonmagnetic and nonquadrupolar ground state, i.e., a singlet as Γ_2 ($W = -1.2$ K, $x = -0.31$).

Figure 2(b) gives the low-temperature dependence of the reciprocal first-order susceptibility: a Curie behavior with a downwards curvature for the magnetic ground state $\Gamma_5^{(1)}$, and a pure Van Vleck one for the nonmagnetic ones, Γ_2 and Γ_3. Without any other complementary data, an experimental Van Vleck behavior may be fitted, varying W and x, with Γ_2 as well as Γ_3 for ground state. Figure 2(c) shows the third-order susceptibility for the $\Gamma_5^{(1)}$ magnetic triplet according to the two mean measurement directions in cubic symmetry. From this example (as from the two others) it is clear that the CEF leads the third-order magnetic susceptibility to be anisotropic. The negative divergence originates from the $-1/T^3$ terms in the expression of $X_0^{(3)}$ given in the Appendix A. The reciprocal cube root of $X_0^{(3)}$, which is the temperature linearized form [inset of Fig. 2(c)] exhibits here some deviations. In addition, its anisotropy changes in sign at about 40 K.

This anisotropic behavior is more emphasized in Fig. 2(d). The inset shows a pure Van Vleck dependence in the case of Γ_2. It arises from (i) the nullity of $\langle \Gamma_2 | J_z | \Gamma_2 \rangle$ which drives the vanishing of the $-1/T^3$ term at low temperature and (ii) the precise cancellation of mixed Van Vleck and Curie terms such as

$$\frac{|\langle \Gamma_2 | J_z | \Gamma_i \rangle|^2 |\langle \Gamma_2 | J_z | \Gamma_j \rangle|^2}{T(E_2 - E_i)(E_2 - E_j)}$$

with terms from $-(X_0^{(1)})^2 / 2T$. The different 0 K values originate from the different triple sums of off-diagonal matrix elements along the two directions.

The case of the Γ_3 doublet as ground state is more exciting [see Fig. 2(d)]. The nullity of diagonal terms, $\langle \Gamma_3 | J_z | \Gamma_3 \rangle$, induces the vanishing of the $-1/T^3$ term at low temperature. But the cancellation observed above in the case of the Γ_2 ground state is found again, but only for the [111] direction. Along the [001] axis, the positive mixed Van Vleck and Curie terms

$$\frac{|\langle \Gamma_3 | J_z | \Gamma_i \rangle|^2 |\langle \Gamma_3 | J_z | \Gamma_j \rangle|^2}{T(E_3 - E_i)(E_3 - E_j)}$$

are dominant, leading to a positive divergence of $X_0^{(3)}$. This has been verified to be a peculiar feature of the Γ_3 doublet. Thus studying the third-order susceptibility may give precise information on the CEF level scheme and appears to be at least as valuable as studying the first-order susceptibility.
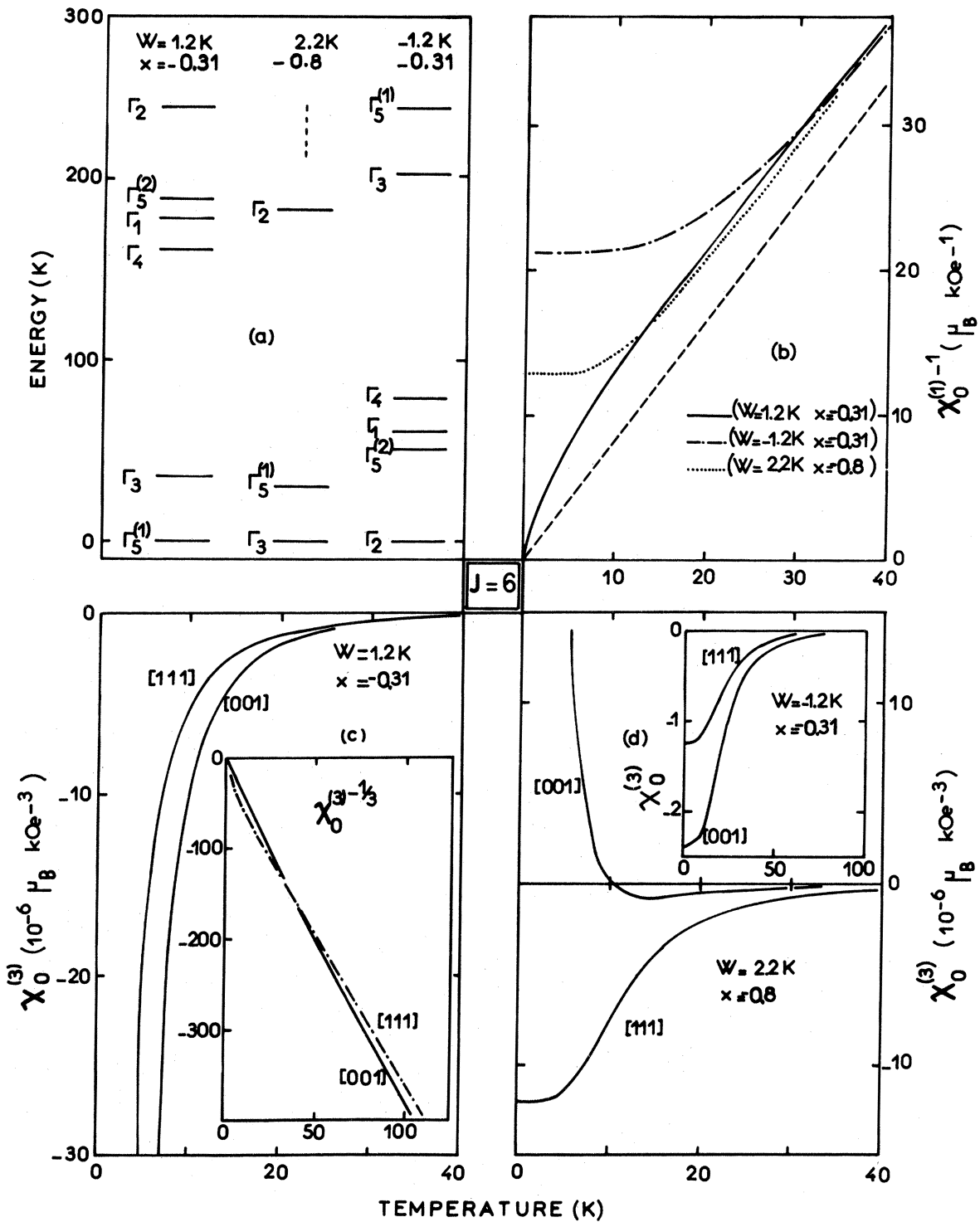
FIG. 2. Calculated temperatures variations of the CEF first- (b) and third-order (c), (d) susceptibilities without any exchange for the three level schemes given in (a). In (b), the hatched straight line is the classical behavior.
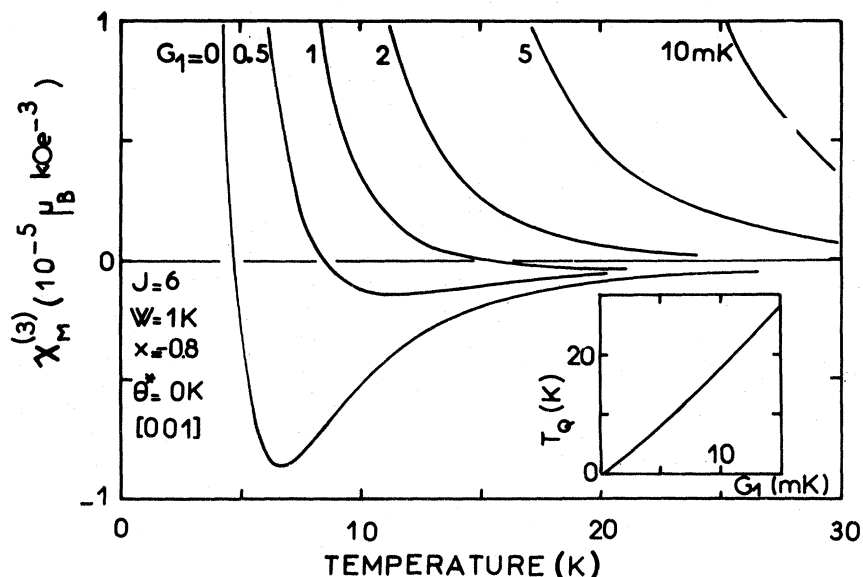
FIG. 3. Calculated temperature variations of the tetragonal third-order susceptibility in presence of quadrupolar interactions and CEF term. The inset gives the quadrupolar ordering as a function of the total quadrupolar coefficient G_1.

3. With CEF and quadrupolar interactions

The effects of the quadrupolar interactions in presence of CEF is obvious in the Fig. 3. The presented curves have been calculated for various G_1 values in absence of bilinear interactions. The nature of the Γ_3 ground state leads to the positive divergence for $G_1 = 0$ as seen above. Increasing G_1 drastically increases the T_0 values in comparison with the Θ_Q^* effect without CEF. For example with $G_1 = 1$ mK, i.e., $\Theta_Q^* = C_Q G_1 = 1.386$ K (with $C_Q = 1386$ for $J = 6$), one finds $T_0 = 15$ K instead of $T_0 = 4.1$ K in the classical model. This is due to the strong quadrupolar character of the Γ_3 doublet.

III. EXPERIMENTAL

In order to obtain experimental values, a possible method may be the analysis of the magnetization curves. Figure 4 shows examples of the isothermal field dependence of the magnetic moment along the fourfold and threefold axes. Plotting M/H vs H^2 may enable us to obtain both the first-order susceptibility, i.e., the isotropic null field value, and the third-order one, i.e., the slope of the linear low-field range. At higher magnetic field, a positive curvature usually occurs in this diagram corresponding to the positive H^5 term in the development of the classical Brillouin function. Fitting the temperature variation of the isotropic first-order susceptibility by using Eq. (4) leads to Θ^*, the bilinear exchange coefficient and fitting the thermal variation of the anisotropic third-order susceptibility leads to the G_1 and G_2 total quad-

rupolar coefficients.

In our study of CsCl-type structure Tm^{3+} compounds, the magnetic field was provided by a superconducting coil, the magnetization measured by a flux magnetometer with an accuracy of 10^{-3} and a sensitivity of 10^{-2} emu. The temperature was stabilized at better than 0.05 K in the range 4.2–30 K. These experimental conditions were clearly better than in a preliminary experiment.[10] A set of experimental data is shown in Fig. 5 for the compound TmCd: at 5 K, which is near the quadrupolar ordering temperature ($T_Q = 3.16$ K) one finds large higher-rank contributions which reduce the linear
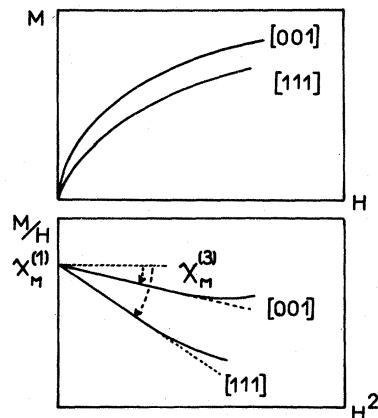
FIG. 4. Analysis of the magnetization field dependence in terms of first- and third-order susceptibilities.
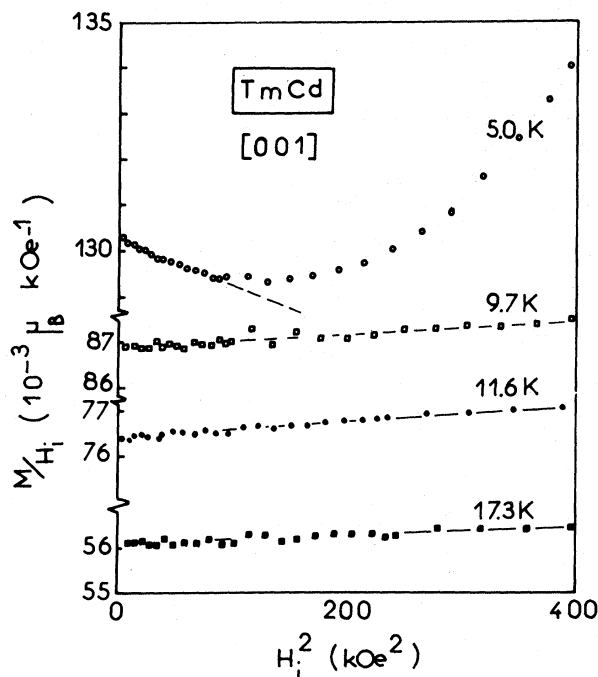
FIG. 5. Plots of $(M/H)(H^2)$ along the fourfold axis in the nonordered range of TmCd.

range; $\chi_M^{(3)}$ is negative. The tetragonal third-order susceptibility increases when increasing the temperature up to positive values ($T = 9.7$ K) before decreasing at higher temperature (11.6 and 17.3 K). In these high-temperature plots, linearity extends up to high fields according to the $(H/T)^3$ ratio occurring in the magnetization field development. The experimental sensitivity does not enable us to observe the excessively high temperature T_0, at which the third-order susceptibility comes back to negative values.

Note that a "dynamical" experimental method, more accurate than this "static" one, may be constituted by the superposition of a small alternating magnetic field of pulsation ω to the static one in order to directly measure the third-order susceptibility through the 3ω flux variation.

IV. APPLICATION TO Tm^{3+} CsCl-TYPE COMPOUNDS

These Tm^{3+} intermetallic compounds have been chosen because many various experiments have shown that the quadrupolar interactions (magnetoelastic coupling and quadrupolar exchange) are particularly large.[2,3] For the Tm^{3+} ion ($J = 6$), the spin moment is small ($S = 1$) with regard to the orbital moment ($L = 5$), and a balanced competition between quadrupolar and bilinear interactions may be expected. We present in this section results obtained

for $\chi_M^{(3)}$ on Tm compounds with copper, cadmium, and zinc, for which a large amount of experimental data exists and which allows us to check the validity of this new method for investigating quadrupolar interactions.

A. TmCu

This compound antiferromagnetically orders at $T_N = 7.7$ K within the $(\pi\pi 0)$-type structure. Its complex magnetic properties at low temperature, as well as all the magnetoelastic properties investigated above T_N, indicate the presence of noticeable quadrupolar interactions.[11,12] The CEF level scheme and wave functions have been deduced from neutron spectroscopy experiments ($W = 1.4$ K, $x = -0.42$). All the CEF susceptibilities, $\chi_0^{(1)}$, $\chi_0^{(3)}$, χ_2, $\chi_2^{(2)}$, are then calculated within this level scheme. Figure 6(a) gives the experimental temperature variation of the reciprocal first-order susceptibility measured along [001] and [111] together with calculated $\chi_0^{(1)-1}(\Theta^* = 0)$. The best agreement is obtained by a simple shift from $\chi_0^{(1)-1}$ to experimental $\chi_M^{(1)-1}$ defined by $\Theta^* = -3.0 \pm 0.3$ K, this value being kept in all the following fits.

The third-order susceptibility measured along [111] is found to be more strongly negative than the behavior, $\chi_0'^{(3)}/(1 - n\chi_0^{(1)})^4$, expected in presence of only bilinear interactions; this indicates a negative trigonal quadrupolar contribution, reinforcing the negative curvature of the magnetization curve. The fit leads to $G_2 = -60 \pm 20$ mK.

Along the fourfold axis, the two contributions are obviously competing: $\chi_M^{(3)}$ is unambiguously positive below 12 K and then vanishes above. Fitting is here particularly selective and leads to $G_1 = 10.3 \pm 0.5$ mK. The calculated curves show that, in absence of antiferromagnetic ordering, $\chi_M^{(3)}$ would decrease down to negative values, the "bilinear type" contribution dominating at low temperature; this will be experimentally observed in TmCd (see Sec. IV B).

B. TmCd and $Tm_{0.3}Y_{0.7}Cd$

TmCd has been extensively studied over the last years.[2,13] It is the first manifestation of a quadrupolar ordering in a cubic rare-earth intermetallic. The quadrupolar exchange interactions drive the tetragonal quadrupolar ordering at $T_Q = 3.2$ K, which is manifested through the tetragonal lattice symmetry lowering through the magnetoelastic coupling.[2] The CEF term is defined by $W = 0.95$ K, $x = -0.34$. The bilinear exchange is zero in TmCd. It is then possible to show the quadrupolar contribution to $\chi_M^{(3)}$ by presenting in the unique Fig. 7 the [001] temperature behavior observed in TmCd and in $Tm_{0.3}Y_{0.7}Cd$,
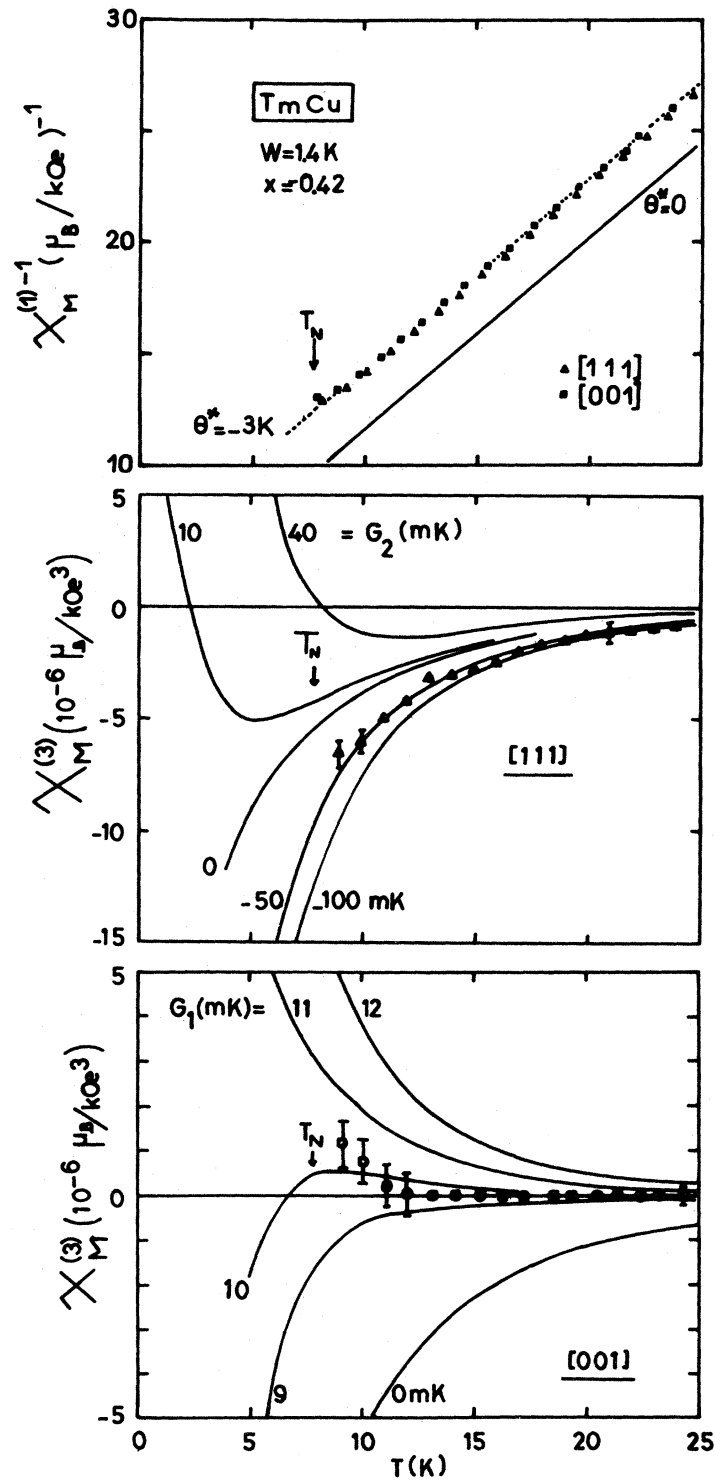
FIG. 6. Reciprocal first-order susceptibility in TmCu (upper part), full and dotted lines result from fits. Temperature variation of the third-order susceptibility along [111] (middle part) and [001] (lower part) full lines are calculated variations and do not account for the occurrence of the antiferromagnetic ordering.
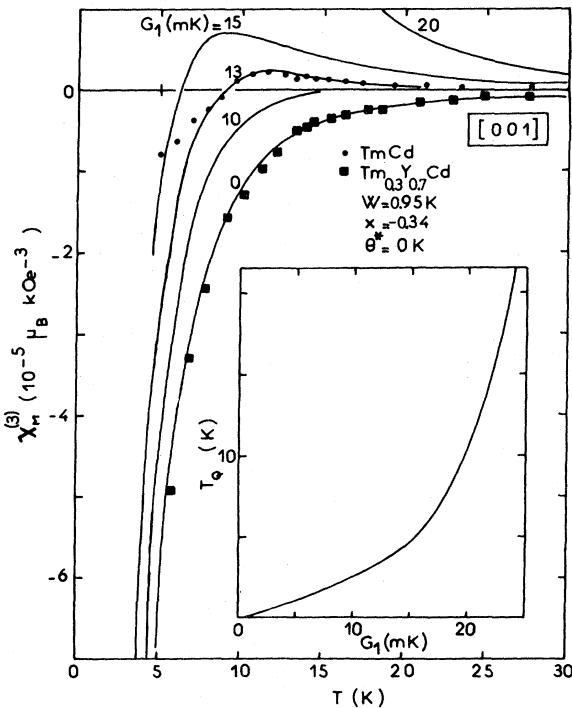
FIG. 7. Temperature dependence of $\chi_M^{(3)}$ along [001] in TmCd and $Tm_{0.3}Y_{0.7}Cd$. Full lines are calculated. The inset gives the quadrupolar ordering temperature, T_Q, as a function of the tetragonal quadrupolar coefficient, G_1.

where the quadrupolar exchange is decreased. The experimental data for the dilute compound always remain negative very close to the behavior calculated without bilinear and quadrupolar interactions ($G_1 \simeq 0$ mK). This agrees with the fact that neither a softening of the ($C_{11} - C_{12}$) mode[14] nor a structural transition was observed above 1.4 K. This indicates the G_1 quadrupolar coefficient rapidly decreases with dilution. In an opposite limit the third-order magnetic susceptibility is unambiguously positive between 9 and 25 K in TmCd and reaches its maximum value at 13 K. Below that temperature, it decreases and changes in sign at 9 K, remaining negative in the low-temperature range, where the negative $\chi_0^{(3)}$ contribution dominates the quadrupolar one. The best fit is obtained with $G_1 = 13 \pm 1$ mK where the discrepancies observed at low temperature may be due to the corrections in vicinity of T_Q. It is indeed difficult to obtain a precise value of $\chi_M^{(3)}$ due to the short linear behavior of $(M/H)(H^2)$ (see Fig. 5). This defect was not observed close to the ordering point in TmCu, $T_N = 7.7$ K, because the magnetization curve in the paramagnetic range, and then $\chi_M^{(3)}$, are not influenced by the antiferromagnetic coupling.

Along the [111] axis, the two sets of data for the two compounds are very close to each other (Fig. 8); the trigonal quadrupolar contribution reinforces the negative curvature. In both cases $G_2 = -50 \pm 10$ mK, and this will be discussed in the last section.
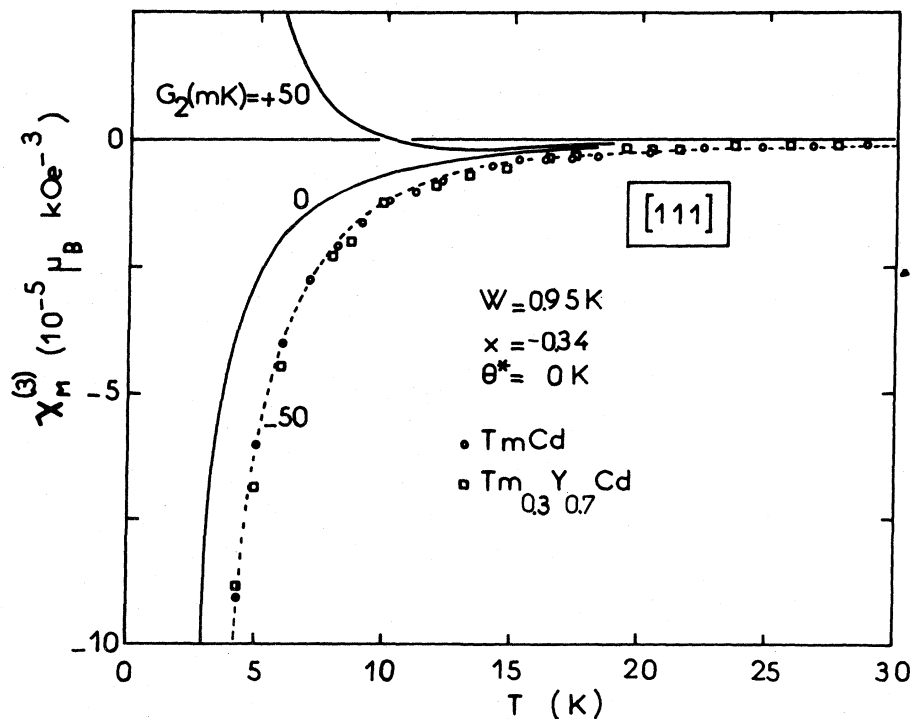
FIG. 8. Temperature dependence of the third-order susceptibility along [111] in TmCd and $Tm_{0.3}Y_{0.7}Cd$; full lines result from fits.

For this [111] symmetry no discrepancy is observed (Fig. 8) close to T_Q, because at T_Q the symmetry lowering mode is tetragonal and not trigonal and therefore no divergence occurs for $\chi_M'^{(3)-1/3}$ along [111].

C. $Tm_\alpha Lu_{1-\alpha} Zn$

TmZn is the second compound, which exhibits a quadrupolar ordering in the paramagnetic phase.[3] Its level scheme is close to the isomorphous TmCd one ($W = 1.2$ K, $x = -0.31$): the $\Gamma_5^{(1)}$ triplet is the cubic ground state which is split at $T_Q = 8.55$ K into a magnetic doublet ($\Gamma_5^{(t)}$ in tetragonal symmetry) and a nonmagnetic singlet ($\Gamma_4^{(t)}$). This singlet, which has a large quadrupolar moment, is the ground state in the tetragonal phase. But in TmZn, the bilinear exchange is large enough to induce a spontaneous moment at $T_c = 8.12$ K. Due to the Van Vleck behavior of this ground state, $\Gamma_4^{(t)}$, this ferromagnetic ordering disappears as soon as a small part of Tm^{3+} is replaced by Lu^{3+} while the quadrupolar ordering remains observable.

In $Tm_{0.7}Lu_{0.3}Zn$ ($T_Q = 3.4$ K), the bilinear exchange is characterized by $\Theta^* = 1.4$ K, deduced from the fit of the reciprocal first-order susceptibility. Along [111], $G_2 = -40 \pm 20$ mK (Fig. 9). Along [001], the quadrupolar interactions are strong enough to dominate the CEF contribution: the third-order susceptibility is positive above 15 K. Above 10 K, fits lead to a G_1 value of about 17 mK, but at lower temperatures, the same discrepancy as found in TmCd occurs again: the experimental data cannot be described with the same G_1 coefficient over the entire temperature range. As T_Q is approached, there are premonitory signs of the transition appearing for this symmetry in $\chi_M^{(3)}$. From the calculated phase diagram $T_Q(G_1)$ (inset of Fig. 9) we can verify that $G_1 = 17$ mK is the value driving a quadrupolar ordering at $T_Q = 3.5$ K, which is very close to the experimental value.

The same bilinear exchange coefficient $\Theta^* = 2.8$ K was found in the nonordered (cubic and paramagnetic) range of $Tm_{0.9}Lu_{0.1}Zn$ and TmZn. Along [111] the effects of the dilution between the three compounds are clear: G_2 increases from -90 mK in TmZn to -70 mK in $Tm_{0.9}Lu_{0.1}Zn$ (Fig. 10) and -40 mK in $Tm_{0.7}Lu_{0.3}Zn$ (Fig. 9).

The situation is more complex for the tetragonal symmetry where the low-temperature discrepancy is obvious. If we restrict the fit to the high-temperature range (Fig. 11), agreement may be found with $G_1 = 23$ mK ($Tm_{0.9}Lu_{0.1}Zn$) and $G_1 = 28$ mK (TmZn). These values lead to calculated T_Q values of 6.4 K and 10.5 K (inset of Fig. 9) which are a little larger than the experimental values of 5.8 and 8.6 K.

In the low-temperature range close to the quadrupolar ordering in both compounds, many explana-
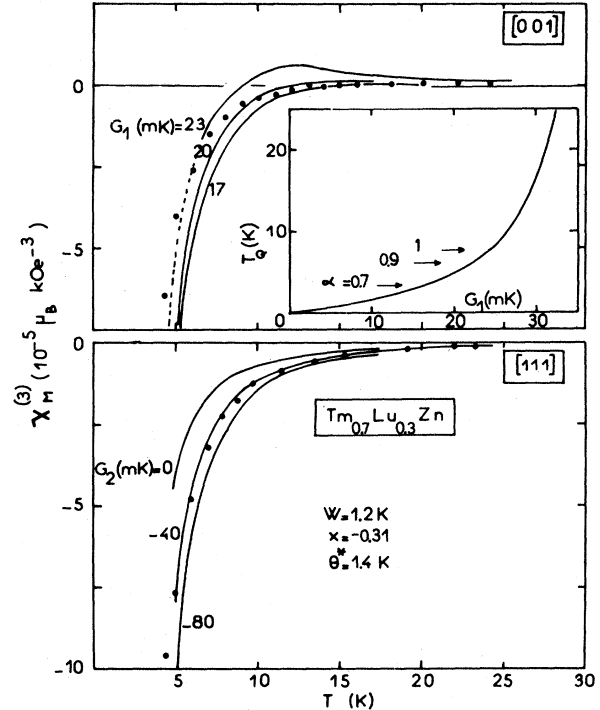
FIG. 9. Temperature variation of $\chi_M^{(3)}$ along [001] (upper part) and [111] (lower part) in $Tm_{0.7}Lu_{0.3}Zn$. The inset gives the calculated quadrupolar ordering temperature T_Q as a function of G_1, the arrows indicate the location of the three studied compounds $Tm_\alpha Lu_{1-\alpha}Zn$; lines are calculated variations.
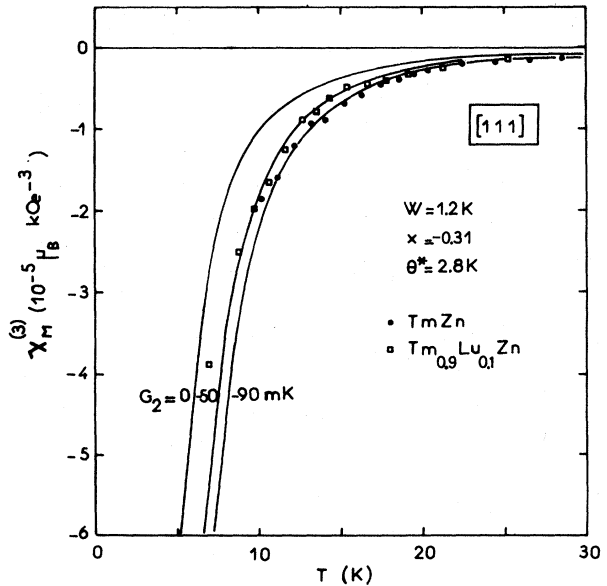
FIG. 10. Temperature variations of $\chi_M^{(3)}$ along [111] in $Tm_{0.9}Lu_{0.1}Zn$ and TmZn (full lines are fitted variations).

P. MORIN AND D. SCHMITT
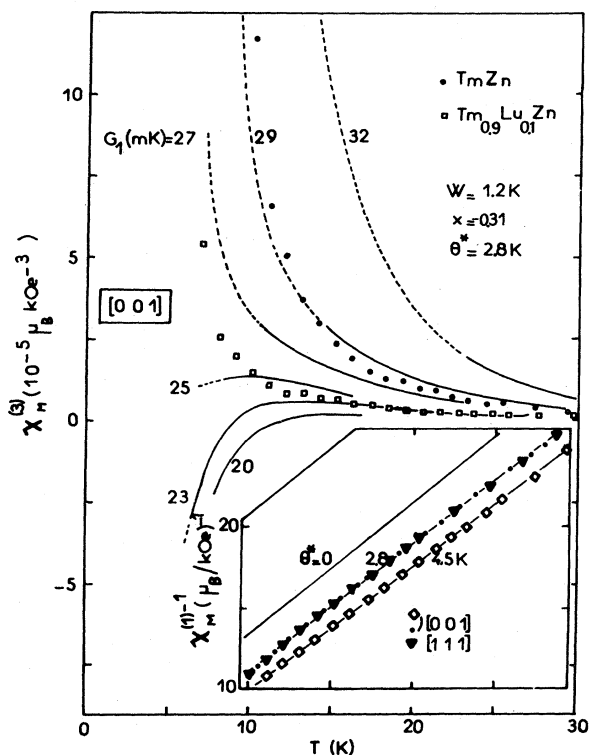
FIG. 11. Temperature variations of $\chi_M^{(3)}$ along [001] in $Tm_{0.9}Lu_{0.1}Zn$ and TmZn. Full lines are calculated variations, they are hatched below T_Q (according to inset of Fig. 9), where the third-order susceptibility cannot be calculated from the same cubic CEF level scheme. The inset gives the temperature behavior of the reciprocal first-order susceptibility measured along [111] (▼) and [001] (◊ from the magnetization curves as explained in the text and ● with a translation balance); lines are calculated variations for various bilinear exchange.

tions may be proposed. First the same one as in TmCd (Sec. IV B) may be valid (coexistence of many competing high-order H/T terms, all influenced by quadrupolar interactions in the vicinity of T_Q). In addition, residual strain effects are important in $Tm_\alpha Lu_{1-\alpha}Zn$ compounds due to the strong tetragonal magnetoelastic coupling, for instance the tetragonal spontaneous strain is -9×10^{-3} in $TmZn^3$ instead of -0.6×10^{-3} in TmCd.[15]

As a consequence each [001] magnetization curve is marked by the past history of the sample during the experimental procedure: at a given temperature T_i, above T_Q, there exists a critical field which drives the sample from the paramagnetic state to the (single domain) ferromagnetic tetragonal state (see Sec. II D of Ref. 3 for a more detailed discussion). Decreasing the field from this latter state leads to a low-field slope, i.e., a first-order susceptibility value, a little stronger than for increasing field. This corresponds

to a sample remaining slightly strained and agrees with calculations which predict a stronger first-order susceptibility in the paramagnetic tetragonal phase. Starting from this slightly strained state, the following isothermal $(T_{i+1} = T_i + 1$ K) magnetization curve exhibits a too large low-field slope. The corresponding [001] $\chi_M^{(1)-1}$ values would lead to $\Theta^* = 4.5$ K (inset of Fig. 11) instead of $\Theta^* = 2.8$ K as deduced from both the [111] $\chi_M^{(1)-1}$ values obtained from the [111] magnetization curves, free of residual trigonal strain effects, and the [001] data obtained in a weak magnetic field with a translation balance. About the third-order susceptibility, this residual strain effect on the bilinear exchange coefficient then strongly reinforces the positive value through $(1 - n\chi_0^{(1)})^4$. Note that in the second experimental method of the Sec. III, working in low (ac) magnetic fields would avoid the effects of this residual strain.

V. CONCLUSION

The G_1 and G_2 parameters determined in these Tm systems are given in Table I with the physical parameters occurring in the fits. About the tetragonal symmetry, the effects of quadrupolar interactions on $\chi_M^{(3)}$ are spectacular, leading to a balanced competition with the $\chi_0^{(3)}$ term and then to precise G_1 determinations. This is particularly true for TmCu where elastic constants, parastriction and magnetization measurements[12] give precise values for the magnetoelastic coupling $[B_1^2/(C_{11}^0 - C_{12}^0) = 4.0 \pm 0.5$ mK] and the quadrupolar exchange $(K_1 = 7.0 \pm 0.5$ mK). The same conclusions remain closely valid for TmCd $[B_1^2/c_{11}^0 - c_{12}^0 = 1.3 \pm 0.3$ mK and $K_1 = 11.2 \pm 1.0$ mK (Ref. 2)]. From the comparison between TmCd and $Tm_{0.3}Y_{0.7}Cd$, the G_1 coefficient seems to quickly decrease with the dilution, in agreement with the vanishing of softening effects in ultrasonic velocity data.[14] In $Tm_{0.7}Lu_{0.3}Zn$, the G_1 value obtained from $\chi_M^{(3)}$ well describes the quadrupolar ordering temperature T_Q as in TmCd.

On the other hand, in $Tm_{0.9}Lu_{0.1}Zn$ and TmZn, the quadrupolar interactions are too large and modify the magnetization field dependence above T_Q mainly through a field hysteresis of the induced tetragonal strain. This shows the shortcomings of our present experimental method, which may imply too large magnetic fields in such specific cases. For these cases, actually low magnetic fields are necessary and better results may be expected from dynamical susceptibility measurements.

The G_2 quadrupolar parameter is always found to be negative. The effects of dilution in $Tm_\alpha Lu_{1-\alpha}Zn$ are obvious, this was not observed in the isomorphous system with Cd. Comparing the G_2/G_1 experimental ratios ranging from -6 to -2 to 12 (the ratio for isotropic quadrupolar interactions) indicates that

TABLE I. Physical parameters occurring into the fits. W and x are deduced from neutron spectroscopy data (except for $Tm_\alpha Y_{1-\alpha} Cd$) and Θ^* from first-order magnetic susceptibility measurements.

| | CEF terms | | Bilinear exchange Θ^* (K) | Total quadrupolar coefficients | |
	W(K)	x		G_1 (mK)	G_2 (mK)
TmCu	1.4	−0.42	−3.0	10.3 ± 0.3	−60 ± 20
TmCd				13 ± 1	−50 ± 20
	0.95	−0.34	0		
$Tm_{0.3}Y_{0.7}Cd$				∼ 0	−50 ± 20
$Tm_{0.7}Lu_{0.3}Zn$			1.4	∼ 17	−40 ± 20
$Tm_{0.9}Lu_{0.1}Zn$	1.2	−0.31	2.8	∼ 23	−70 ± 20
TmZn			2.8	∼ 28	−90 ± 20

the trigonal quadrupolar interactions are clearly the weakest ones in the CsCl-type structure compounds. *This third-order susceptibility study allows the first determination of G_2, which had not been achieved from ultrasonic velocity[2] and parastriction[6] data* because of the weakness of the magnetoelastic coupling compared to the quadrupolar exchange for trigonal symmetry, for instance $B_2^2/4C_{44}^0 = 1.6 \pm 1$ mK while $G_2 = -60 \pm 20$ mK in TmCu.[12]

This analytical study of the anisotropic third-order magnetic susceptibility appears from Sec. II as a possible way of determination of CEF terms. In addition to its anisotropic feature, the observation of a change of sign of $\chi_0^{(3)}$ in its temperature dependence appears to be of importance; it may enable us to choose between two level schemes with nonmagnetic ground states, e.g., one with the Γ_3 doublet, the other with Γ_1 or Γ_2 singlet. Such a choice is impossible from the analysis of the only first-order susceptibility.[16]

The third-order susceptibility study is very fruitful in obtaining information about quadrupolar interactions. Performed in the nonordered (cubic and paramagnetic) range it allows determinations of the two total quadrupolar coefficients for the tetragonal and trigonal symmetries, whatever the low-temperature ordered structure is. It then constitutes a complementary determination besides the ultrasonic velocity and parastriction measurements. However, it necessitates both single crystals and good experimental conditions. As for fitting the high-field magnetization processes, it neglects the magnetic band contribution which may be expected to be weak in Tm compounds as verified in a polarized neutron diffraction experiment in TmZn.[17] A study of the whole RZn series is underway which will check this particular point as well as provide determinations for the two symmetry coefficients G_1 and G_2 throughout the series.

APPENDIX A

In a first step we define the eigenvalues E_i and the eigenvectors $|ik\rangle$ corresponding to the crystal-field Hamiltonian $\mathcal{H}_{CEF}$:

$$\mathcal{H}_{CEF}|ik\rangle = E_i|ik\rangle \quad . \tag{A1}$$

In each subspace i the eigenfunctions $|ik\rangle$ have to be adapted to the perturbation Hamiltonian. A perturbation theory up to the second order for ϵ_3 and the fourth order for H allows us to obtain the analytical expressions of the perturbed energies E_{ik}

$$E_{ik} = E_i + \sum_{n=1}^{4} E_{ik}^{(n)} + \cdots \quad . \tag{A2}$$

Then the partition function Z

$$Z = \sum_{i,k} e^{-\beta E_{ik}} \tag{A3}$$

can be calculated, where $\beta = 1/k_B T$, k_B is the Boltzmann constant and T is the temperature. One obtains

$$Z = Z_{CEF}\{1 + \tfrac{1}{2}\beta\chi_0^{(1)}H^2 + \tfrac{1}{2}\beta\chi_2(B_1\epsilon_3)^2 + \beta\chi_2^{(2)}B_1\epsilon_3 H^2$$

$$+ \tfrac{1}{4}\beta[\chi_0^{(3)} + \tfrac{1}{2}\beta(\chi_0^{(1)})^2]H^4 + \cdots\} \quad , \tag{A4}$$

which leads to the expression of the total free energy $F_{tot} = -k_B T \ln Z$ given in [Eq. (10)].

The expression of the four CEF susceptibilities χ_0, χ_2, $\chi_2^{(2)}$, and $\chi_0^{(3)}$ are given by

$$\chi_0^{(1)} = g_J^2 \mu_B^2 \sum_{i,k} f_i \left[-2 \sum_{j \neq i,l} \frac{|J_{ik,jl}|^2}{E_i - E_j} + \frac{1}{k_B T} |J_{ik,ik}|^2 \right] \ , \tag{A5}$$

$$\chi_2 = \sum_{i,k} f_i \left[-2 \sum_{j \neq i,l} \frac{|Q_{ik,jl}|^2}{E_i - E_j} + \frac{1}{k_B T} |Q_{ik,ik}|^2 \right] \ , \tag{A6}$$

$$\chi_2^{(2)} = g_J^2 \mu_B^2 \sum_{i,k} f_i \left[\sum_{j \neq i,l} \sum_{j' \neq i,l'} \frac{J_{ik,jl} Q_{jl,j'l'} J_{j'l',ik} + 2 Q_{ik,jl} J_{jl,j'l'} J_{j'l',ik}}{(E_i - E_j)(E_i - E_{j'})} \right.$$
$$\left. - \sum_{j \neq i,l} \frac{|J_{ik,jl}|^2 Q_{ik,ik} + 2 Q_{ik,jl} J_{jl,ik} J_{ik,ik}}{(E_i - E_j)} \left[\frac{1}{E_i - E_j} + \frac{1}{k_B T} \right] + \frac{1}{2(k_B T)^2} |J_{ik,ik}|^2 Q_{ik,ik} \right] \ , \tag{A7}$$

$$\chi_0^{(3)} = -\frac{1}{2 k_B T} (\chi_0)^2 + g_J^4 \mu_B^4 \sum_{i,k} f_i \left[-4 \sum_{\substack{j \neq i,l \\ j' \neq i,l' \\ j'' \neq i,l''}} \frac{J_{ik,jl} J_{jl,j'l'} J_{j'l',j''l''} J_{j''l'',ik}}{(E_i - E_j)(E_i - E_{j'})(E_i - E_{j''})} \right.$$
$$+ 2 \sum_{\substack{j \neq i,l \\ j' \neq i,l'}} \frac{|J_{ik,jl}|^2 |J_{ik,j'l'}|^2 + 2 J_{ik,jl} J_{jl,j'l'} J_{j'l',ik} J_{ik,ik}}{(E_i - E_j)(E_i - E_{j'})} \left[\frac{2}{E_i - E_j} + \frac{1}{k_B T} \right]$$
$$\left. - 2 \sum_{j \neq i,l} \frac{|J_{ik,ik}|^2 |J_{ik,jl}|^2}{(E_i - E_j)} \left[\frac{2}{(E_i - E_j)^2} + \frac{2}{(E_i - E_j) k_B T} + \frac{1}{k_B^2 T^2} \right] + \frac{1}{6 k_B^3 T^3} |J_{ik,ik}|^4 \right] \ , \tag{A8}$$

where

$$J_{ik,jl} = \langle ik | J_z | jl \rangle \tag{A9}$$

and

$$Q_{ik,jl} = \langle ik | O_2^0 | jl \rangle \tag{A10}$$

are the matrix elements of J_z and O_2^0 between the cubic CEF levels. For each degenerate CEF level i,

$$f_i = \frac{1}{Z_{CEF}} e^{-\beta E_i} = e^{-\beta E_i} \Big/ \sum_{i,k} e^{-\beta E_i} \tag{A11}$$

is the Boltzmann population factor.

APPENDIX B

When the magnetic field H is applied along a threefold axis, e.g., [111], the rhombohedral symmetry implies that the nonzero average values are in the fourfold axis system:

$$\langle J_x \rangle = \langle J_y \rangle = \langle J_z \rangle \ , \quad \langle P_{xy} \rangle = \langle P_{yz} \rangle = \langle P_{zx} \rangle \ ,$$

and

$$\epsilon_{xy} = \epsilon_{yz} = \epsilon_{zx} \ .$$

It is then more convenient to make a rotation of the coordinates axes so that [111] is the new z axis. In the new system

$$M' = g_J \mu_B \langle J_z \rangle$$

and

$$Q' = \langle O_2^0 \rangle$$

are the only nonzero expectation values and the new Hamiltonain and corresponding free energy are written as

$$\mathcal{H}' = \mathcal{H}_{CEF} - g_J \mu_B (H + nM') J_z - \tfrac{1}{2} B_2 \epsilon_{kl} O_2^0 - \tfrac{1}{12} K_2 Q' O_2^0 + [6 C_{44}^0 (\epsilon_{kl})^2 + \tfrac{1}{2} nM'^2 + \tfrac{1}{24} K_2 Q'^2] \ ,$$

$$F'_{tot} = F'_{CEF} - \tfrac{1}{2} \chi_0^{(1)} (H + nM')^2 - \tfrac{1}{2} \chi_2' (\tfrac{1}{2} B_2 \epsilon_{kl} + \tfrac{1}{12} K_2 Q')^2$$
$$- \chi_2^{(2)'} (\tfrac{1}{2} B_2 \epsilon_{kl} + \tfrac{1}{12} K_2 Q')(H + nM')^2 - \tfrac{1}{4} \chi_0^{(3)'} (H + nM')^4 + 6 C_{44}^0 \epsilon_{kl}^2 + \tfrac{1}{2} nM'^2 + \tfrac{1}{24} K_2 Q'^2 \ .$$

Here $\chi_0^{(1)'} = \chi_0^{(1)}$ because of the isotropy of the first-order magnetic susceptibility in cubic symmetry. χ_2', $\chi_2^{(2)'}$, and $\chi_0^{(3)'}$ have the same expressions as the corresponding tetragonal susceptibilities, but their values differ from the nonprimed susceptibilities according to the new cubic CEF wave functions in the new axes system adapted to the rhombohedral symmetry. The equilibrium conditions for M', ϵ_{kl}, and Q' lead to

$$M' = \chi_M^{(1)'} H + \chi_M^{(3)'} H^3 + \cdots \quad ,$$

$$\epsilon_{kl} = \frac{B_2}{24 C_{44}^0} Q' \quad ,$$

$$Q' = \chi_Q' H^2 + \cdots \quad ,$$

with

$$\chi_M^{(1)'} = \frac{\chi_0^{(1)}}{1 - n\chi_0^{(1)}} = \chi_M^{(1)} \quad ,$$

$$\chi_M^{(3)'} = \frac{\chi_0^{(3)'}}{(1 - n\chi_0^{(1)})^4} + \frac{1}{6} G_2 \frac{(\chi_2^{(2)'})^2}{(1 - n\chi_0^{(1)})^4 (1 - \frac{1}{12} G_2 \chi_2')} \quad ,$$

$$\chi_Q' = \frac{\chi_2^{(2)'}}{(1 - n\chi_0^{(1)})^2 (1 - \frac{1}{12} G_2 \chi_2')} \quad ,$$

and the total trigonal quadrupolar coefficient

$$G_2 = \frac{(B_2)^2}{4 C_{44}^0} + K_2 \quad .$$

*Laboratoire propre du CNRS, associé à l'Université Scientifique et Médicale de Grenoble.

[1]P. M. Levy, P. Morin, and D. Schmitt, Phys. Rev. Lett. 42, 1417 (1979).

[2]R. Aleonard and P. Morin, Phys. Rev. B 19, 3868 (1979).

[3]P. Morin, J. Rouchy, and D. Schmitt, Phys. Rev. B 17, 3684 (1978).

[4]P. Morin and D. Schmitt, J. Phys. F 8, 951 (1978).

[5]M. E. Mullen, B. Lüthi, P. S. Wang, E. Bucher, L. D. Longinotti, J. P. Maita, and H. R. Ott, Phys. Rev. B 10, 186 (1974).

[6]P. Morin, D. Schmitt, and E. du Tremolet de Lacheisserie, Phys. Rev. B 21, 1742 (1980).

[7]R. L. Melcher, "The Anomalous Elastic Properties of Materials Undergoing Cooperative Jahn-Teller Phase Transitions," *Physical Acoustics*, edited by W. P. Mason and R. N. Thruston (Academic, New York, 1975), Vol. XII.

[8]K. H. J. Buschow, H. W. de Wijn, and A. M. van Diepen, J. Chem. Phys. 50, 137 (1969).

[9]K. R. Lea, M. J. M. Leask, and W. P. Wolf, J. Phys. Chem. Solids 23, 1381 (1962).

[10]P. Morin and D. Schmitt, Phys. Lett. 73A, 67 (1979).

[11]P. Morin and D. Schmitt, J. Magn. Magn. Mater. 21, 243 (1980).

[12]C. Jaussaud, P. Morin, and D. Schmitt, J. Magn. Magn. Mater. 22, 98 (1980).

[13]B. Lüthi, M. Muller, K. Andres, E. Bucher, and J. P. Maita, Phys. Rev. B 8, 2639 (1973).

[14]B. Lüthi (private communication).

[15]H. R. Ott and K. Andres, Solid State Commun. 15, 1341 (1974).

[16]B. R. Cooper, Helv. Phys. Acta 41, 750 (1968).

[17]D. Givord, P. Morin, and D. Schmitt (unpublished).